

Beyond the Standard Model Kaon Mixing with physical light quarks

Julia Kettle¹

Peter Boyle¹, Nicolas Garron², Renwick Hudspith³, Ava Khamseh¹,
Tobias Tsang¹

RBC-UKQCD

¹University of Edinburgh ²University of Liverpool ³York University

Lattice 2018, July 2018

The RBC & UKQCD collaborations

BNL and BNL/RBRC

Yasumichi Aoki (KEK)
Mattia Bruno
Taku Izubuchi
Yong-Chull Jang
Chulwoo Jung
Christoph Lehner
Meifeng Lin
Aaron Meyer
Hiroshi Ohki
Shigemi Ohta (KEK)
Amarjit Soni

UC Boulder

Oliver Witzel
Columbia University

Ziyuan Bai
Norman Christ
Duo Guo
Christopher Kelly
Bob Mawhinney
Masaaki Tomii
Jiqun Tu
Bigeng Wang

Tianle Wang
Evan Wickenden
Yidi Zhao
University of Connecticut

Tom Blum
Dan Hoying (BNL)
Luchang Jin (RBRC)
Cheng Tu

Edinburgh University

Peter Boyle
Guido Cossu
Luigi Del Debbio
Tadeusz Janowski
Richard Kenway
Julia Kettle

Fionn O'haigan
Brian Pendleton
Antonin Portelli
Tobias Tsang
Azusa Yamaguchi

KEK

Julien Frison

University of Liverpool

Nicolas Garron

MIT

David Murphy
Peking University

Xu Feng

University of Southampton

Jonathan Flynn
Vera Guelpers
James Harrison
Andreas Juettner
James Richings
Chris Sachrajda

Stony Brook University

Jun-Sik Yoo
Sergey Syritsyn (RBRC)

York University (Toronto)

Renwick Hudspith

Table of contents

1 Introduction

2 Lattice Implementation

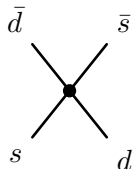
3 Analysis

4 Results

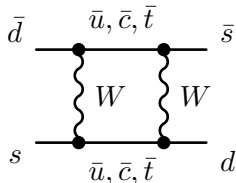
5 Summary

Kaon Mixing in the Standard Model

- Oscillation of K^0 to \bar{K}^0
- One-loop FCNC
- Mediated by W^\pm
- Related to indirect CP violation



$$O^{\Delta S=2} = [\bar{s}_a \gamma_\mu (1 - \gamma_5) d_a] [\bar{s}_b \gamma_\mu (1 - \gamma_5) d_b]$$



- OPE separates out a long-distance 4quark operator
- Matrix elements of $O^{\Delta S=2}$ calculated with LQCD

Beyond the Standard Model

Generalized Weak Hamiltonian:

$$\mathcal{H}^{\Delta S=2} = \sum_{i=1}^5 C_i(\mu) O_i + \sum_{i=1}^3 \tilde{C}_i(\mu) \tilde{O}_i$$

Basis of 5 model independent parity-even four-quark operators.

$$O_1 = [\bar{s}_a \gamma_\mu (1 - \gamma_5) d_a] [\bar{s}_b \gamma_\mu (1 - \gamma_5) d_b]$$

$$O_2 = [\bar{s}_a (1 - \gamma_5) d_a] [\bar{s}_b (1 - \gamma_5) d_b]$$

$$O_3 = [\bar{s}_a (1 - \gamma_5) d_b] [\bar{s}_b (1 - \gamma_5) d_a]$$

$$O_4 = [\bar{s}_a (1 - \gamma_5) d_a] [\bar{s}_b (1 + \gamma_5) d_b]$$

$$O_5 = [\bar{s}_a (1 - \gamma_5) d_b] [\bar{s}_b (1 + \gamma_5) d_a]$$

Past calculations by SWME¹, ETM² and RBC-UKQCD³.

¹Jang et al 15, Bae et al 14

²Carrasco et al 15, Bertone et al 10

³Garron, Hudspith, Lytle 16, Blum et al 14

Simulations

- 2+1f DWF QCD with Iwasaki Gauge Action
- 3 lattice spacings
- 2 ensembles with physical pions
- New: $a^{-1} = 2.774 \text{GeV}$ $m_\pi \approx 230 \text{MeV}$

name	L/a	T/a	kernel	source	$a^{-1}[\text{GeV}]$	$m_\pi[\text{MeV}]$	n_{configs}	am_l^{uni}	am_s^{sea}	am_s^{val}	am_s^{phys}
C0	48	96	M	Z2GW	1.7295(38)	139	90	0.00078	0.0362	0.0358	0.03580(16)
C1	24	64	S	Z2W	1.7848(50)	340	100	0.005	0.04	0.03224	0.03224(18)
M0	64	128	M	Z2GW	2.3586(70)	139	82	0.000678	0.02661	0.0254	0.02539(17)
M1	32	64	S	Z2GW	2.3833(86)	303	83	0.004	0.03	0.02477	0.02477(18)
M2	32	64	S	Z2GW	2.3833(86)	360	76	0.006	0.03	0.02477	0.02477(18)
F1	48	96	M	Z2GW	2.774(10)	234	98	0.002144	0.02144	0.02132	0.02132(17)

M and F stand for coarse, medium and fine, respectively, M and S for Moebius and Shamir kernels. Propagators had either Z2 wall (Z2W) or Z2 Gaussian Wall (Z2GW) sources, with latter including source smearing.

Simulations

- 2+1f DWF QCD with Iwasaki Gauge Action
- 3 lattice spacings
- 2 ensembles with physical pions
- New: $a^{-1} = 2.774 \text{GeV}$ $m_\pi \approx 230 \text{MeV}$

name	L/a	T/a	kernel	source	$a^{-1}[\text{GeV}]$	$m_\pi[\text{MeV}]$	n_{configs}	am_l^{uni}	am_s^{sea}	am_s^{val}	am_s^{phys}
C0	48	96	M	Z2GW	1.7295(38)	139	90	0.00078	0.0362	0.0358	0.03580(16)
C1	24	64	S	Z2W	1.7848(50)	340	100	0.005	0.04	0.03224	0.03224(18)
M0	64	128	M	Z2GW	2.3586(70)	139	82	0.000678	0.02661	0.0254	0.02539(17)
M1	32	64	S	Z2GW	2.3833(86)	303	83	0.004	0.03	0.02477	0.02477(18)
M2	32	64	S	Z2GW	2.3833(86)	360	76	0.006	0.03	0.02477	0.02477(18)
F1	48	96	M	Z2GW	2.774(10)	234	98	0.002144	0.02144	0.02132	0.02132(17)

M and F stand for coarse, medium and fine, respectively, M and S for Moebius and Shamir kernels. Propagators had either Z2 wall (Z2W) or Z2 Gaussian Wall (Z2GW) sources, with latter including source smearing.

Simulations

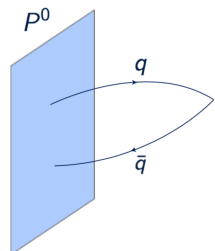
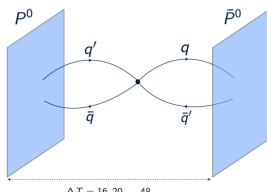
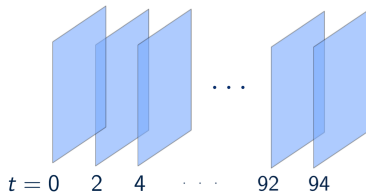
- 2+1f DWF QCD with Iwasaki Gauge Action
- 3 lattice spacings
- 2 ensembles with physical pions
- New: $a^{-1} = 2.774 \text{GeV}$ $m_\pi \approx 230 \text{MeV}$

name	L/a	T/a	kernel	source	$a^{-1}[\text{GeV}]$	$m_\pi[\text{MeV}]$	n_{configs}	am_l^{uni}	am_s^{sea}	am_s^{val}	am_s^{phys}
C0	48	96	M	Z2GW	1.7295(38)	139	90	0.00078	0.0362	0.0358	0.03580(16)
C1	24	64	S	Z2W	1.7848(50)	340	100	0.005	0.04	0.03224	0.03224(18)
M0	64	128	M	Z2GW	2.3586(70)	139	82	0.000678	0.02661	0.0254	0.02539(17)
M1	32	64	S	Z2GW	2.3833(86)	303	83	0.004	0.03	0.02477	0.02477(18)
M2	32	64	S	Z2GW	2.3833(86)	360	76	0.006	0.03	0.02477	0.02477(18)
F1	48	96	M	Z2GW	2.774(10)	234	98	0.002144	0.02144	0.02132	0.02132(17)

M and F stand for coarse, medium and fine, respectively, M and S for Moebius and Shamir kernels. Propagators had either Z2 wall (Z2W) or Z2 Gaussian Wall (Z2GW) sources, with latter including source smearing.

Source-Sink Time Separations

- Z_2 (Gaussian) wall sources at every other time slice.
- Several different ΔT
- Bin all data with same ΔT



Quantities Measured

The SM bag parameters:

$$B_1(\mu) = \frac{\langle \bar{P} | \mathcal{O}_1(\mu) | P \rangle}{\frac{8}{3} m_K^2 f_K^2} \quad B_{i>1}(\mu) = \frac{(m_s(\mu) + m_d(\mu))^2}{N_i m_K^4 f_K^2} \langle \bar{P} | \mathcal{O}_i(\mu) | P \rangle$$

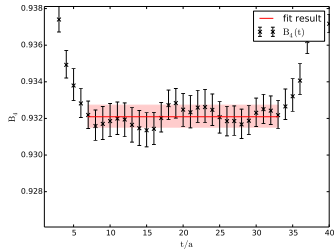
Define a ratio parameter:

$$R_i\left(\frac{m_P^2}{f_P^2}, a^2, \mu\right) = \left[\frac{f_K^2}{m_K^2}\right]_{exp} \left[\frac{m_P^2}{f_P^2} \frac{\langle \bar{P} | \mathcal{O}_i(\mu) | P \rangle}{\langle \bar{P} | \mathcal{O}_1(\mu) | P \rangle}\right]_{lat}$$

such that when $a^2 \rightarrow 0$ and $m_P^2/f_P^2 \rightarrow m_K^2/f_K^2$ it reduces to:

$$R_i(\mu) = \frac{\langle \bar{K} | \mathcal{O}_i(\mu) | K \rangle}{\langle \bar{K} | \mathcal{O}_1(\mu) | K \rangle}$$

Correlator Fitting



(a) $\mathcal{B}_4(t)$ for C0

$$\frac{C_{2pt}^{3pt}(t, t_{sink})}{C_{2pt}^{AP}(t)C_{2pt}^{AP}(t_{sink}-t)} \rightarrow \frac{\langle \bar{P}|O_i|P\rangle}{\langle P|A\rangle\langle A|P\rangle}$$

(b) $\mathcal{R}_5(t)$ for M0.

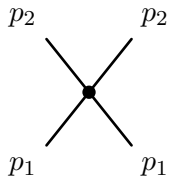
$$\frac{C_i^{3pt}(t, t_{sink})}{C_1^{3pt}(t, t_{sink})} \rightarrow \frac{\langle \bar{P}|O_i|P\rangle}{\langle \bar{P}|O_1|P\rangle}$$

Examples of the fits of correlation functions to measure lattice quantities.

Non-Perturbative Renormalisation

- We use the Rome-Southampton method with non-exceptional kinematics (RI-SMOM).

$$O_i(\mu)^{\overline{MS}} = C_{ij}^{\overline{MS} \leftarrow MOM}(\mu) \left(\lim_{a^2 \rightarrow 0} \frac{Z_{jk}^{RI}(\mu)}{Z_q^2} O_k(a) \right)$$



$$Z^{RI}(\mu) \hat{P}[\Lambda(p^2)]|_{p^2=\mu^2} = \Lambda(p^2)^{tree}$$

$$p_1 \neq p_2$$

$$p_1^2 = p_2^2 = (p_1 - p_2)^2$$

Non-Perturbative Renormalisation

- Block diagonal structure due to chiral symmetry

$$Z_{O^{\Delta S=2}} = \begin{pmatrix} Z_{11} & 0 & 0 & 0 & 0 \\ 0 & Z_{22} & Z_{23} & 0 & 0 \\ 0 & Z_{32} & Z_{33} & 0 & 0 \\ 0 & 0 & 0 & Z_{44} & Z_{45} \\ 0 & 0 & 0 & Z_{54} & Z_{55} \end{pmatrix}$$

- Define two intermediate schemes (γ, γ) and $(\not\!\!\gamma, \not\!\!\gamma)$ distinguished by their projectors. The difference between them allows us to quantify a systematic error

Extrapolation to Physical Point and Continuum

Simultaneously extrapolate to the continuum and chiral limit in a global fit with form:

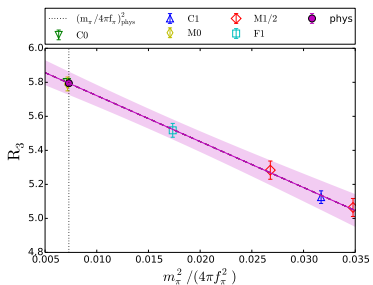
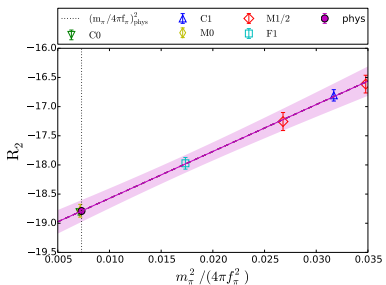
$$Y\left(a^2, \frac{m_{ll}^2}{f_{ll}^2}, \delta_{m_s^{sea}}\right) = Y\left(0, \frac{m_\pi^2}{f_\pi^2}, 0\right) \left[1 + \alpha_i a^2 + \beta_i \frac{m_{ll}^2}{f_{ll}^2} + \gamma_i \delta_{m_s^{sea}}\right]$$

where we include a term linear strange sea-quark mass:

$$\delta_{m_s^{sea}} = \frac{(m_s^{sea} - m_s^{phys})}{m_s^{phys}}$$

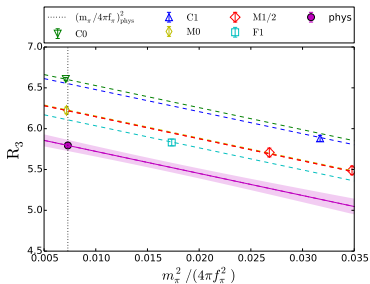
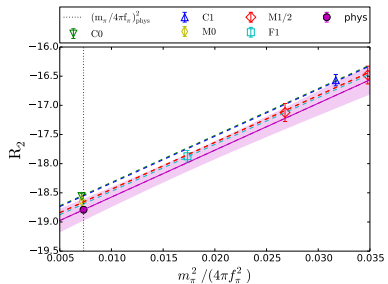
Ratio Parameter Fits

Figure: Preliminary results for R_2 and R_3 in \overline{MS} at 3 GeV RI-SMOM $^{\gamma,\gamma}$ intermediate scheme. Data points have been adjusted to the physical strange-mass and continuum using the fit form and parameters gained from the fit.



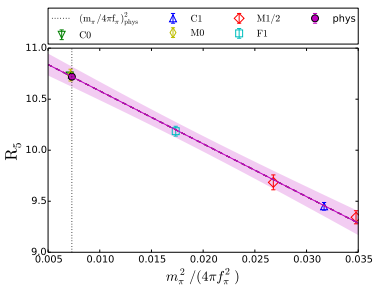
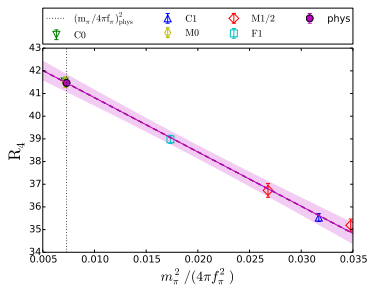
Ratio Parameter Fits (not corrected to continuum)

Figure: Preliminary results for R_2 and R_3 in \overline{MS} at 3 GeV
RI-SMOM $^{(\gamma,\gamma)}$ intermediate scheme.



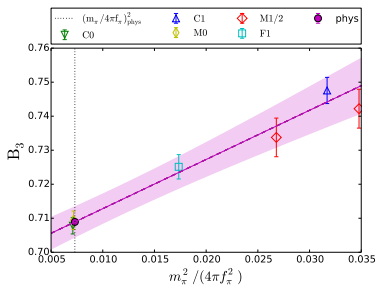
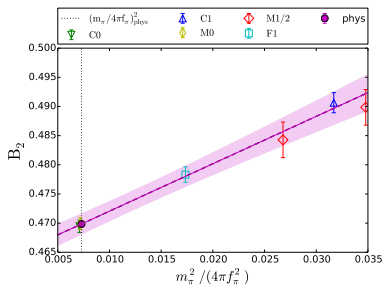
Ratio Parameter Fits

Figure: Preliminary results for R_4 and R_5 in \overline{MS} at 3 GeV RI-SMOM $^{\gamma,\gamma}$ intermediate scheme. Data points have been adjusted to the physical strange-mass and continuum.



Bag Parameter Fits

Figure: Preliminary results for B_2 and B_3 in \overline{MS} at 3 GeV RI-SMOM $^{\gamma,\gamma}$ intermediate scheme. Data points have been adjusted to the physical strange-mass and continuum.



Bag Parameter Fits

Figure: Preliminary results for B_4 and B_5 in \overline{MS} at 3 GeV RI-SMOM $^{\gamma,\gamma}$ intermediate scheme. Data points have been adjusted to the physical strange-mass and continuum.

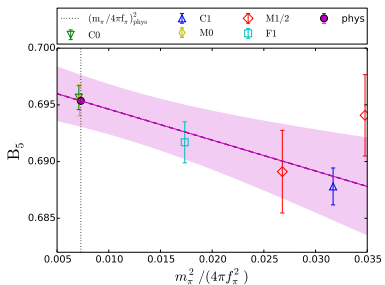
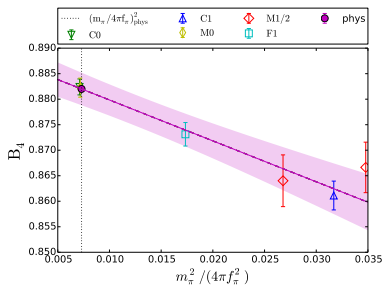


Table of Results

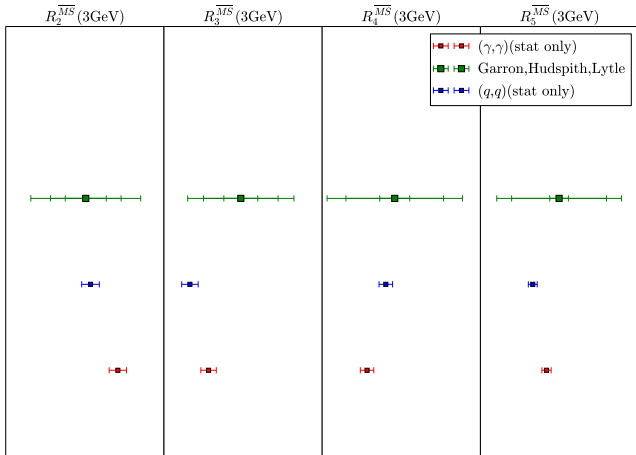
Physical point continuum limit results - with stat error only

		-	R_2	R_3	R_4	R_5
SMOM	(γ, γ)	-	-18.50(18)	5.529(64)	38.59(37)	10.9(10)
	(q, q)	-	-19.83(19)	5.416(71)	41.12(39)	10.427(96)
$\overline{\text{MS}}$	(γ, γ)	-	-18.79(19)	5.795(68)	41.46(40)	10.720(99)
	(q, q)	-	-19.38(19)	5.630(73)	42.58(40)	10.424(95)
		B_1	B_2	B_3	B_4	B_5
SMOM	(γ, γ)	0.5156(12)	0.5125(20)	0.7509(49)	0.9088(33)	0.7789(28)
	(q, q)	0.5337(12)	0.5115(17)	0.6667(54)	0.9002(29)	0.6968(23)
$\overline{\text{MS}}$	(γ, γ)	0.5177(12)	0.4699(18)	0.7089(46)	0.8820(32)	0.6954(23)
	(q, q)	0.5289(12)	0.4741(16)	0.6555(55)	0.8839(27)	0.6610(21)

Values of χ^2/dof

		-	R_2	R_3	R_4	R_5
MOM	(γ, γ)	-	0.05	0.07	0.97	0.40
	(q, q)	-	0.01	0.15	0.73	0.38
ms	(γ, γ)	-	0.09	0.14	0.96	0.40
	(q, q)	-	0.01	0.16	0.75	0.38
		B_1	B_2	B_3	B_4	B_5
MOM	(γ, γ)	1.86	1.36	2.37	0.52	0.92
	(q, q)	1.34	1.59	5.74	0.43	1.63
ms	(γ, γ)	1.84	0.63	1.50	1.20	1.87
	(q, q)	1.32	1.43	6.08	0.57	2.17

Comparison with Previous Results



PT error $\approx 2\%$

Comparison with Previous Results

Consistency within errors with previous results.

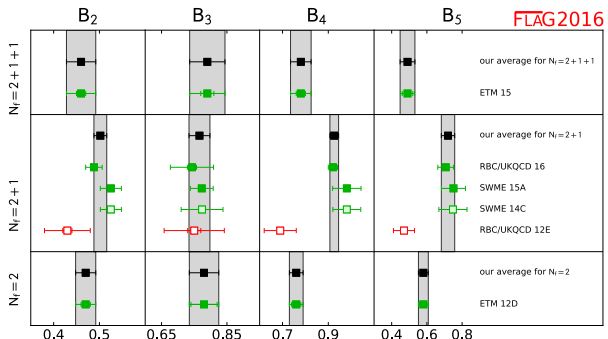
	this work	RBC-UKQCD14 ⁴	RBC-UKQCD16 ⁵
$B_K^{(q,q)}(\overline{\text{MS}}, 3\text{GeV})$	0.5289(12)	0.5293(17)(106)	0.536(9)(6)(11)
$R_2^{(\gamma,\gamma)}(\overline{\text{MS}}, 3\text{GeV})$	-18.79(19)	-	-19.48(44)(32)(42)
$R_3^{(\gamma,\gamma)}(\overline{\text{MS}}, 3\text{GeV})$	5.795(68)	-	6.08(15)(18)(14)
$R_4^{(\gamma,\gamma)}(\overline{\text{MS}}, 3\text{GeV})$	41.5(40)	-	43.11(89)(201)(112)
$R_5^{(\gamma,\gamma)}(\overline{\text{MS}}, 3\text{GeV})$	10.720(99)	-	10.99(20)(82)(32)

Stat error improved significantly.

⁴Blum et al, 2014, arXiv:1411.7017

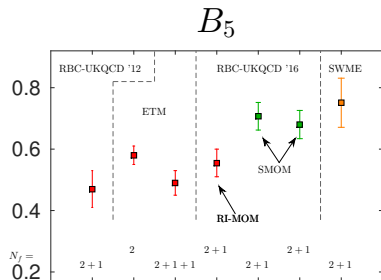
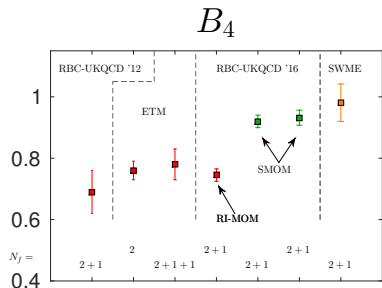
⁵Garron, Hudspith, Lytle, 2016, arXiv:1609.03334

Tensions in previous results



Tensions in previous results

In Garron et al⁶ it was proposed that source of tension come from choice of kinematics in renormalisation.



⁶Garron et al, RBC-UKQCD, 16 arXiv:1609.03334

Summary

- Two times smaller statistical error
- Third lattice spacing in fit
- Data directly at physical point for first time
- Systematic error will be dominated by perturbation theory
- Quantify truncation in perturbation theory by difference between schemes
- Consistent with previous RBC-UKQCD results with NE schemes
- Exceptional schemes remain in disagreement (pion pole model suspect)

Acknowledgements

Thanks to all members of RBC-UKQCD for their weekly discussions and comments.

Backup slides

Figure: Preliminary results for R_2 and R_3 in \overline{MS} at 3 GeV
 RI-SMOM $^{(\gamma,\gamma)}$ intermediate scheme.

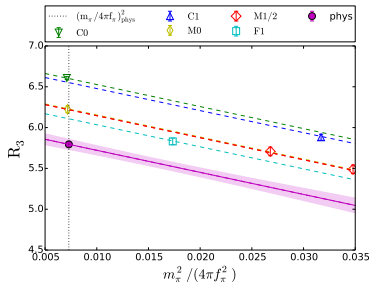
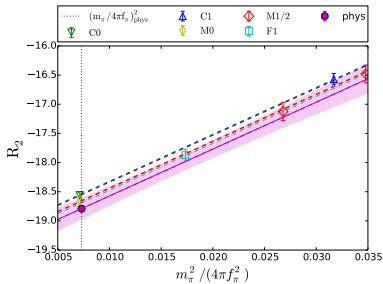


Figure: Preliminary results for R_4 and R_5 in \overline{MS} at 3 GeV
 RI-SMOM $^{(\gamma,\gamma)}$ intermediate scheme.

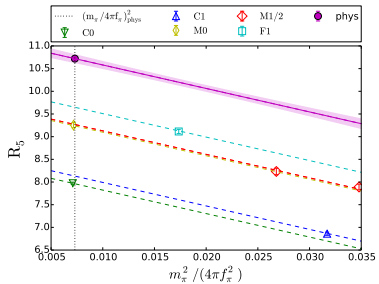
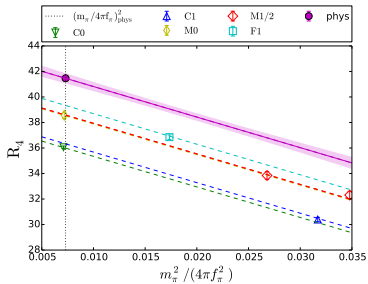


Figure: Preliminary results for B_2 and B_3 in \overline{MS} at 3 GeV
 RI-SMOM $^{(\gamma,\gamma)}$ intermediate scheme.

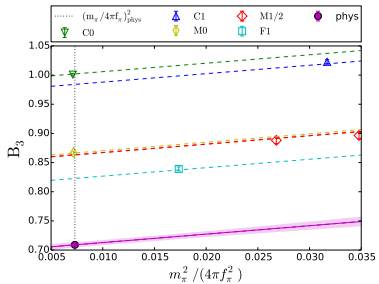
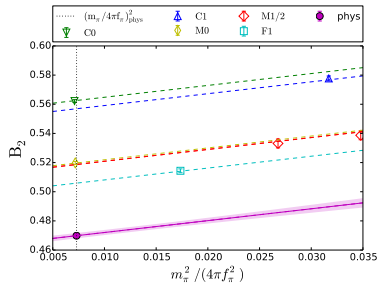
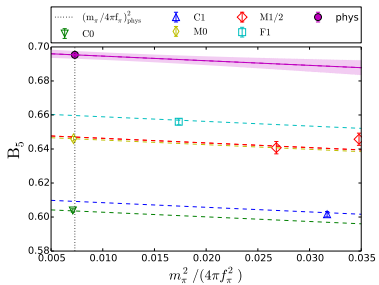
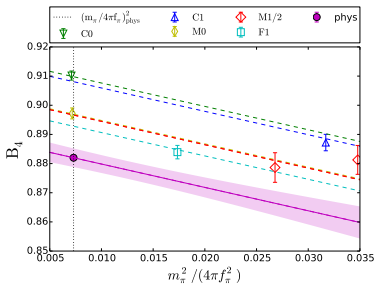
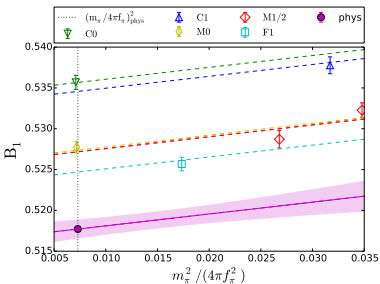
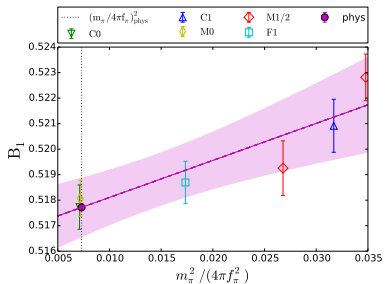


Figure: Preliminary results for B_4 and B_5 in \overline{MS} at 3 GeV RI-SMOM $^{(\gamma,\gamma)}$ intermediate scheme.



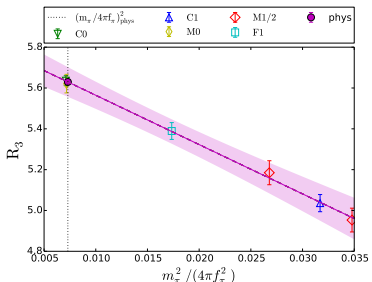
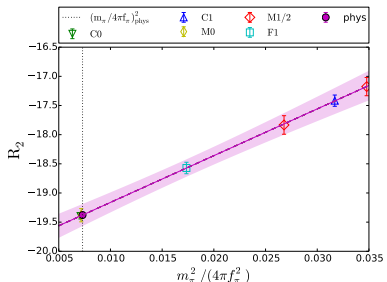
SM Bag parameter

Figure: Preliminary results for B_K in \overline{MS} at 3 GeV RI-SMOM $^{(\gamma,\gamma)}$ intermediate scheme.



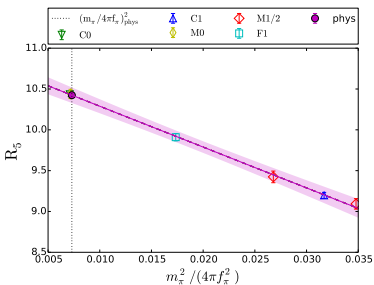
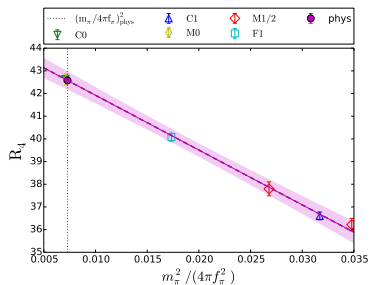
Results - (q, q)

Figure: Preliminary results for R_2 and R_3 in \overline{MS} at 3 GeV
RI-SMOM (q, q) intermediate scheme.



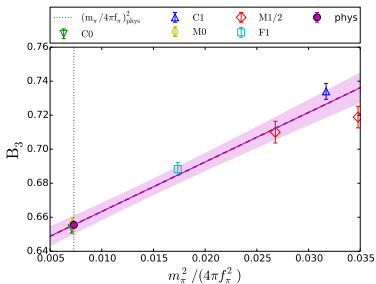
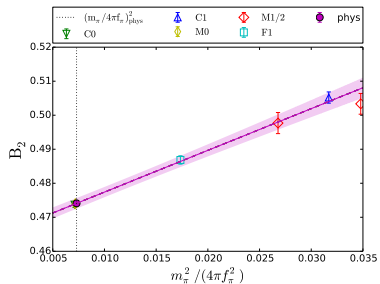
Results - (q, \bar{q})

Figure: Preliminary results for R_4 and R_5 in \overline{MS} at 3 GeV
RI-SMOM $^{q,\bar{q}}$ intermediate scheme.



Results - (q, \bar{q})

Figure: Preliminary results for B_2 and B_3 in \overline{MS} at 3 GeV
RI-SMOM q, \bar{q} intermediate scheme.



Results - (q, \bar{q})

Figure: Preliminary results for B_4 and B_5 in \overline{MS} at 3 GeV
RI-SMOM q, \bar{q} intermediate scheme.

